Tree-ring indicators of German summer drought over the last millennium

Ulf Büntgen [a,b,*], Valerie Trouet [a], David Frank [a], Hanns Hubert Leuschner [c], Dagmar Friedrichs [d], Jürg Luterbacher [e], Jan Esper [f]

[a] Swiss Federal Research Institute WSL, Zürcherstrasse 111, 8903 Birmensdorf, Switzerland
[b] Oeschger Centre for Climate Change Research (OCCR), University of Bern, 3012 Bern, Switzerland
[c] Georg-August-University, Department of Palynology and Climate Dynamics, Wilhelm-Weber-Str. 2a, Göttingen 37073, Germany
[d] Department of Geography, University of Bonn, Meckenheimer Allee 166, Bonn 53115, Germany
[e] Department of Geography, Justus-Liebig-University, Senckenbergstrasse 1, Giessen 35390, Germany
[f] Department of Geography, Johannes Gutenberg University, Becherweg 21, Mainz 55099, Germany

ARTICLE INFO

ABSTRACT

Past natural and future anthropogenic drought variability has and will impact terrestrial ecosystems, agricultural productivity, socio-economic conditions, and public health on various time-scales. In comparison to reconstructed and projected temperature change, much less is known about variations in the hydrological cycle. Here we present 953 living and historical oak (*Quercus* sp) ring width samples from Central Germany (51–52°N and 9–10°E), that span the AD 996–2005 period and explain ~18–70% of inter-annual to decadal scale June–September drought variance at the regional-scale. Driest and wettest summers common to the tree-ring proxy and instrumental target data are 1934, 1959, 1996 and 1958, 1966, 1967, respectively. Spatial field correlations are positive with gridded summer hydro-climate over western-central Europe. Increased mid-tropospheric geopotential height (Z500) anomalies over the British Isles appear associated with increased Central German drought, whereas negative Z500 anomalies over Western Europe trigger wet summer extremes due to anomalous moist air advection from the west. Although our study revealed estimates of inter-annual to decadal drought dynamics at the synoptic scale, lower frequency trends remain insecure.

© 2010 Elsevier Ltd. All rights reserved.

1. Introduction

Much progress has recently been made in deriving annually resolved estimates of hydro-climatic fluctuations over the last centuries to millennia. Besides various reconstructions of regional-scale precipitation and/or drought variability (see references herein), a prominent network of tree-ring width (TRW) data from the contiguous United States of America (Cook et al., 2004) allowed hydro-climatic blueprints of the Medieval Climate Anomaly (MCA; ~800–1300) to be identified (Seager et al., 2007). Such information is of particular interest as the MCA represents the closest natural analogue to recent modifications of the hydrological cycle, characterized by mid-latitudinal precipitation increases and subtropical drought (Cook et al., 2007; Huntington, 2006). While the MCA was most likely attributed to increased solar irradiance and La Niña-like climate states (Trouet et al., 2009 and references therein), recent conditions are forced by anthropogenic emissions (Zhang et al., 2007).

On the European-scale, annually resolved estimates of pre Little Ice Age (LIA; Grove 1988) hydro-climatic conditions are restricted to TRW data from southern Finland (Helama et al., 2009), northern Africa (Esper et al., 2007), and the eastern Mediterranean (Touchan et al., 2005). Central European records, however, rarely extend beyond the LIA and contain overall weaker climate signals (Brázdil et al., 2002; Wilson et al., 2005; Büntgen et al., 2009). At the same time, various studies have proven drought sensitivity of living (Friedrichs et al., 2009a,b), and historical oak chronologies (Kelly et al., 1989, 2002). The potential of sub-fossil bog oaks to cover periods of several millennia has also been outlined (Leuschner et al., 2002). Their dendroclimatological potential, however, depends on a convincing separation of climatologically and non-climatologically induced signals on longer than annual time-scales (see Haneca et al., 2009 for a review).

We here present a study that overcomes some of these limitations related to sample provenance and climate sensitivity to reconstruct German drought variability over the last millennium. We, therefore, compiled 953 living and historical oak TRW series from a well-defined area in Central Germany. We attempted to preserve high- to low-frequency information back into medieval

* Corresponding author. Tel.: +41 44 739 2679; fax: +41 44 739 2215.
E-mail address: buentgen@wsl.ch (U. Büntgen).

times by adequate data replication, and investigations of influences of tree-ring detrending approaches. Uncertainty, synoptic variability, and long-term behavior of the new reconstruction are discussed to emphasize future research priorities.

2. Materials and methods

2.1. Tree-ring data, detrending, and chronology development

The most drought sensitive cluster out of a total of 555 living oaks (*Quercus* sp) was selected (see Friedrichs et al., 2009a for details). This cluster contains 63 trees from four locations within a well-defined area (51–52°N and 9–10°E) in Central Germany (Northern Hesse and Lower Saxony), and represents the species-specific biome center (Fig. 1A–B). All trees grew on slopes between 5 and 40% inclination, below 550 m asl, and on pure cambi- and luvisols. The sample area is predominantly influenced by maritime atmospheric air masses from the North Atlantic sector, but rain shadow effects of the western German mountain ranges together with Eurasian high-pressure cells can cause frequently occurring soil-moisture changes during the vegetation period (Friedrichs et al., 2009b). Mean annual temperature of the 20th century was 7.8 °C with values of ~15 °C between June and September (Fig. 1C). Annual precipitation totals of ~700 mm were evenly distributed throughout the year. June–September (JJAS) temperature means (15 °C), precipitation totals (9.7 mm/day), and drought indices (scPDSI = 0.3) fluctuated without significant long-term trends over the past century (Fig. 1D). High temperature means and average precipitation totals, however, triggered relatively dry conditions during the 1940s (Friedrichs et al., 2009b).

To extend the living data back in time, samples of 890 historical oak timbers from the same area in Northern Hesse and Lower Saxony were selected from a pan-European network of several thousand oaks (Kelly et al., 2002). We preferred to use fewer data (i.e., 890) from a well-defined region where timber provenancing guaranteed that the historical samples match the living sites, rather than utilizing the abundant oak pool (of thousands of samples and a complex noise component inherent to such compilations). The spatial restriction yielded ecological agreement between the living and historical subset. All samples were collected from construction timbers of ancient frame houses and church-roof frameworks. Clearly defined parish boundaries since medieval times, persisting management rules, sufficient wood supply, and poor floating conditions allow provenancing of the herein considered oak timbers, and also constrain the ecological boundary of past forest sites (B. Leuschner, personal communication).

The resulting (living and historical) composite of ~135,300 annually resolved TRW measurements from 953 oak samples covers the AD 996–2005 period (Fig. 2). Samples are characterized by internal coherence over most of the past millennium: the mean inter-series correlation (Rbar) is 0.29 and the mean Expressed Population Signal (EPS) is 0.93 (Fig. 2A). This common variance within the TRW series implies a climatic control upon regional oak growth. Sample replication peaks during the 16th century (~250 series; Fig. 2B, D). Mean segment length remains fairly stable during the last millennium at ~150 years, but mean tree age constantly increases from ~1000 to 1250, 1300 to 1700, and again during the 20th century. The living and historical data correlate at $r = 0.5$ ($p < 0.01$) over their common 1841–1871 period (>10 series per subset chronology). Even though the observed agreement is only based on a short overlap between mature (historical) and juvenile (living) wood, it is stronger than previously reported relationships ($r = 0.4$) amongst different oak sites in Central Germany (Friedrichs et al., 2009b). EPS statistics of 0.93 at the living/historical subset transition range above the frequently applied quality threshold of 0.85, and indicate that a theoretical population (for this species and region) is well represented (Wigley et al., 1984).

To test for varying frequency preservation in the TRW chronologies, individual cubic smoothing splines with 50% frequency–response cutoff equaling 300 years (300SP), negative exponential
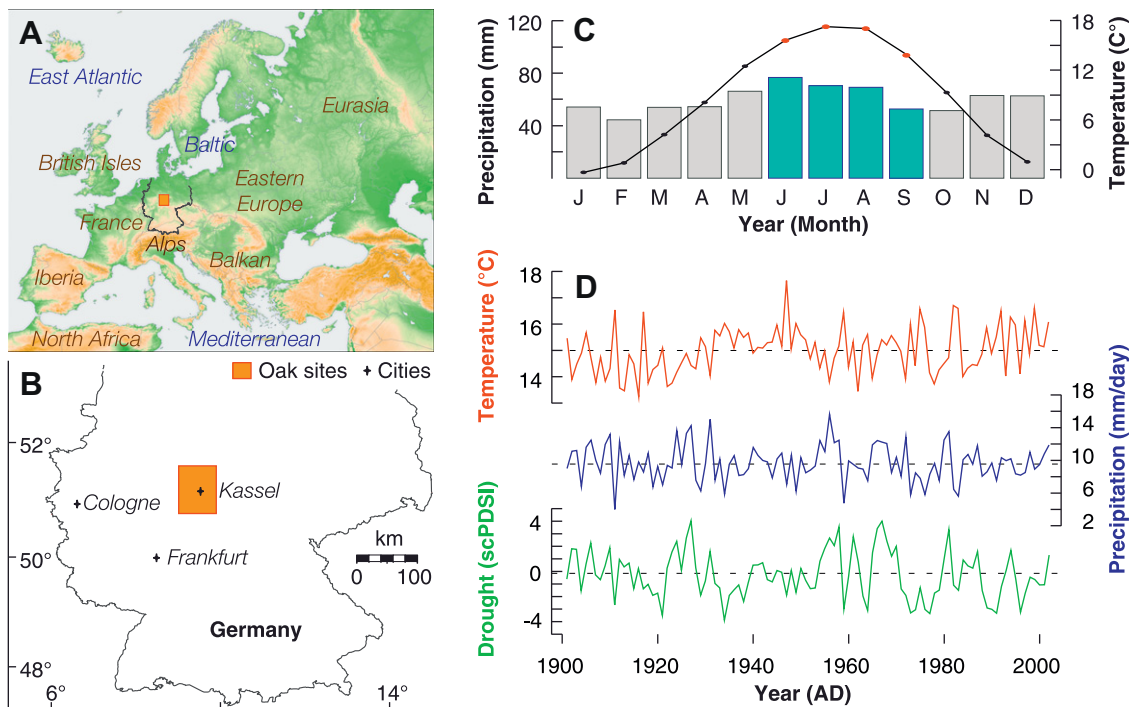
Fig. 1. Geographical setting: location of the study site within (A) Europe and (B) Germany (orange box indicates the sampling region and the instrumental grid-box data used). (C) Climate diagram (with respect to 1961–90 and colors referring to the June–September period of maximum tree growth), and (D) 20th century JJAS temperature, precipitation and drought variability averaged over the 8.5–9.5°E and 51.0–52.0°N region (CRUTS2.1; Mitchell and Jones, 2005).
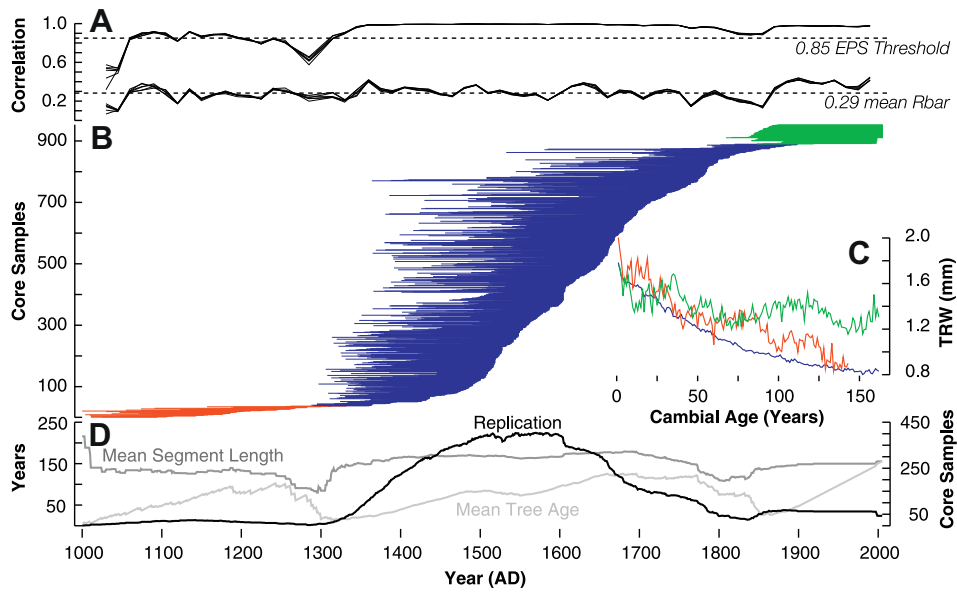
Fig. 2. Data characteristic: (A) 31-year moving Rbar and EPS statistics after six different detrendings: 300sp, 300spPT, NEG, NEGPT, RCS, RCSPT of (B) the 953 TRW samples, sorted by their outermost ring and split into living (63 series), historical (853 series) and early (37 series) subsets. (C) Their Regional Curves (RCs) with replication >10 series, and (D) the temporal evolution of mean segment length, sample replication, and mean tree age.

functions (NEG), and the Regional Curve Standardization (RCS; Esper et al., 2003) were applied to both raw and power-transformed measurements (Cook and Peters, 1981, 1997). We aimed at preserving high- to low-frequency information in the final TRW record, but due to differences in growth levels and age trends between the living and historical samples (Fig. 2C, Table 1), series were (horizontally) split into living (63), historical (853), and early (37) populations for RCS detrending (Büntgen et al., 2005, 2006, 2008). Without performing this horizontal splitting, we obtained a strong positive trend in recent growth that did not match the trend of the instrumental records. Their weighted mean after variance stabilization (Frank et al., 2007b) was used as the final drought proxy (hereafter RCS chronology). Note that even though the horizontal split approach may reduces long-term biases in the RCS chronology, it can diminish lower frequency information within in the shorter early and living subsets, which only span three and two centuries, respectively (see Cook et al., 1995 for details), as well as between the subsets, which are set to the same mean and variance.

Other techniques of chronology development were employed to add details on the high- to low-frequency variance that can be retained in the combined oak data (Frank et al., 2007b). Comparison of the 300SP, NEG, and RCS detrended chronologies shows various levels of frequency maintenance (Fig. 3). Time-series after individual detrending contain a whiter spectrum, whereas the RCS chronology reflects more reddish processes. Inter-annual to decadal-scale variability with peak values in the 19th century and

between ∼1250 and 1400, however, persists amongst the different detrending methods applied. Commonly preserved high- to mid-frequency information is emphasized by mean correlations of 0.99 and 0.95 after 20-year high-pass and 20–60-year band-pass filtering the different chronology versions. Mean correlation of 0.69 between the three chronologies after 60-year low-pass filtering indicates increasing differences in the lower frequencies, which appeared to be substantial during the 19th century, ∼1540, and prior to ∼1350.

Large positive growth anomalies towards the MCA-LIA transition (e.g., 1350–1370) – a feature that appeared independent of the tree-ring detrending method applied (Fig. 4) – were additionally evaluated (via subset chronology development) to ensure their robustness. The 1350–1370 growth anomaly occurred during a period without an abrupt shift in sample replication, since the number of oak samples steadily increased from 20 series in 1320 to 323 series in 1450 (Fig. 4A). A subset chronology of only those 23 oak series that started before 1330 and ended after 1400 was developed for additional verification (Fig. 4B). The resulting record appeared to be unaffected by the inclusion of juvenile (faster growing) wood.

2.2. Meteorological data and calibration trials

A gridded (0.5° × 0.5°) version of the self-calibrated Palmer Drought Severity Index (scPDSI; van der Schrier et al., 2006) was used as predictor variable for growth response analysis, model calibration, and spatial field correlation over the 1901–2002 period. Monthly anomalies (with respect to 1961–1990) from the four closest grid points to the study area (centered over 51.57°N and 8.75°E, 51.75°N and 9.25°E, 51.25°N and 8.75°E, 51.25°N and 9.25°E) were considered to minimize the influence of differences between single grid-boxes (Fig. 1B) – and possible instrumental targets (Frank et al., 2007a). Correlation coefficients between the tree-ring proxy and instrumental target data were computed over different periods and using moving windows to assess temporal stability. Time-series were high-, low-, and band-pass filtered to assess potential frequency dependence in proxy/target relationships (see Büntgen et al., 2006 for methodological details).

Table 1
Data summary: sample replication, period covered, mean segment length (MSL), average growth rate (AGR), inter-series correlation (Rbar), and the Expressed Population Signal (EPS; Wigley et al., 1984) of the three horizontal subsets and their mean. Rbar and EPS values were computed over 30-year windows lagged by 15 years after RCS detrending.

Sub-sets	Series	Start	End	Period	MSL	AGR	Rbar	EPS
Living	63	1809	2005	197	149	1.47	0.37	0.96
Historical	853	1288	1898	611	143	1.28	0.26	0.96
Early	37	996	1331	336	113	1.48	0.25	0.79
All	953	996	2005	1010	142	1.31	0.29	0.93
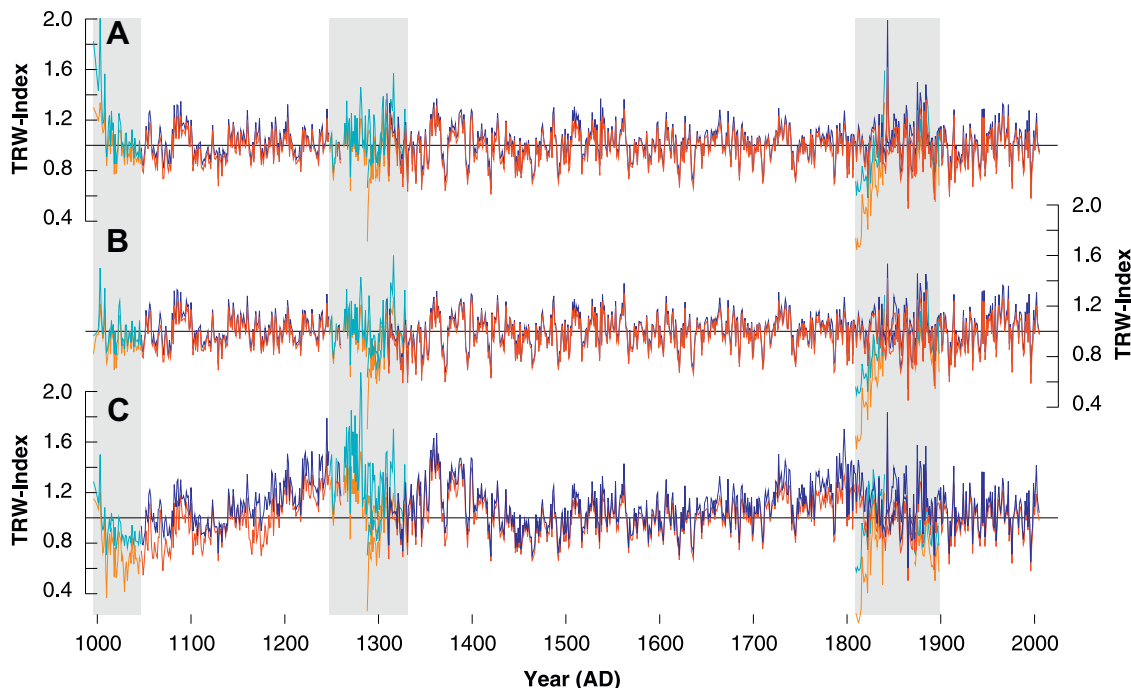
Fig. 3. Chronology development: minimum (red) and maximum (blue) values of 12 slightly different chronologies (considering six techniques of chronology development in combination with ratios or residuals after power-transformation for index calculation) using (A) 300SP, (B) NEG, and (C) RCS detrending for the three horizontal subsets (living, historical, early). Light colors indicate subset transition periods of low replication (<10 series).

To avoid regression-based variance reduction in the model and to best capture the full range of natural drought variability, the RCS chronology was scaled, i.e., mean and variance were adjusted, to the contemporaneous scPDSI indices. This procedure is the simplest amongst various calibration techniques but is also perhaps least prone to variance underestimation (Esper et al., 2005). Spatial field correlations between the drought reconstruction and gridded precipitation, drought, and cloud-cover indices (Mitchell and Jones, 2005) were computed for the European/North Atlantic sector (30–70°N and 10°W–40°E land only), with the cloud-cover data restricted to 1950 to present. Composite analyses were performed for the 20 (10) driest and wettest summers over the pre-instrumental 1659–1900 (instrumental 1901–1999) interval using gridded mid-tropospheric 500 hPa geopotential height (Z500)

reconstructions (Luterbacher et al., 2002). Gridded 2.5° × 2.5° field indices of Z500 were available at monthly (seasonal) resolution back to 1659 (1500) for the 70–30°N and 30°W–40°E region. A combination of instrumental station temperature, precipitation, and pressure series, as well as documentary proxy evidences was used to develop the gridded data (e.g., Brázdil et al., 2005; Luterbacher et al. 2002). Various calibration/verification exercises and industrial/pre-industrial transfer functions confirmed statistical robustness of the mid-tropospheric fields back to the mid 17th century (Luterbacher et al., 2002). For details about the reconstruction technique, the sources of the predictor data, and the uncertainties, we refer to Luterbacher et al. (2002). The methodology for the reconstruction is based on the assumption of stationarity. Thus, the statistically derived relationships between the combined station time-series
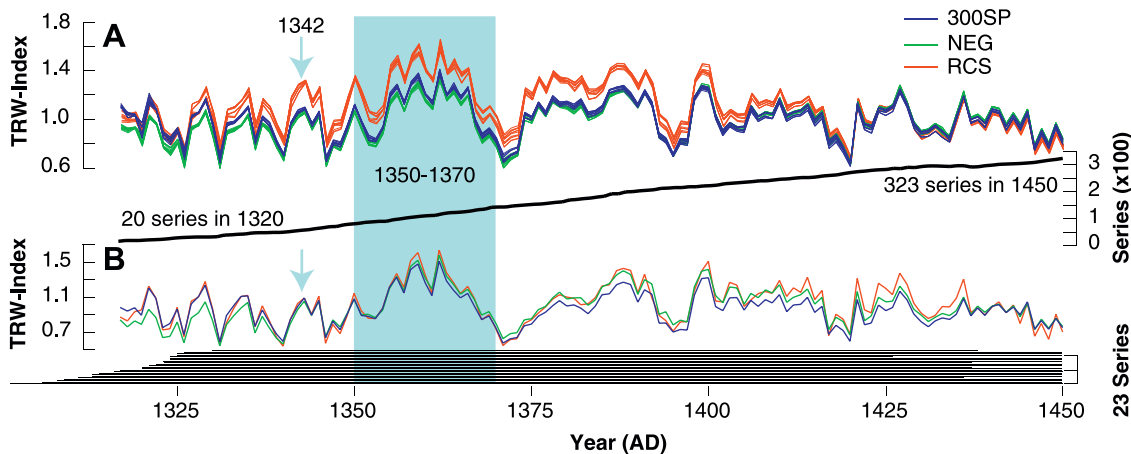
Fig. 4. Growth validation: (A) TRW chronologies after different detrending and chronology development techniques (Fig. 3) and their sample replication. (B) Subset chronologies of 23 individual TRW samples that start before AD 1330 and end after 1400. Blue shading highlights the AD 1350–1370 growth increase, and the blue arrow refers to the summer precipitation event discussed in Dotterweich and Bork (2007) and Bork and Kranz (2008).
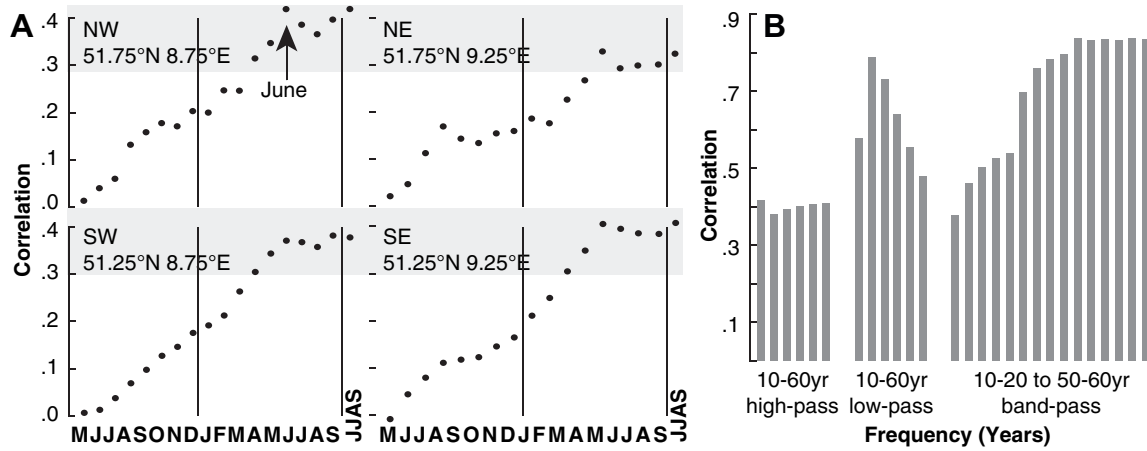
Fig. 5. Drought response: (A) correlations between regional-scale drought variability (scPDSI from four 0.5° × 0.5° grid-cells) and the RCS chronology computed over the 1901–2002 period and using monthly means from previous year May to current year September, plus the seasonal June–September mean. Horizontal grey shadings denote 99% significance corrected for *lag-1* autocorrelation. (B) Correlations (1901–2002) between (low-, high-, and band-pass filtered) JJAS drought variability (scPDSI from the grid-cell centered over 51.75°N and 8.75°E) and the RCS chronology.

and the large-scale Z500 fields over the calibration period are propagated throughout the reconstruction period.

3. Results

3.1. Climate sensitivity

Correlation of the RCS chronology against the four closest scPDSI grid-boxes revealed significant ($p < 0.01$) correlations for monthly values from April to September and the JJAS growing season means (Fig. 5A). Correlations with previous year drought conditions were non-significant. Spatial response patterns were generally negligible, but the grid-box northwest of the study site – representing the main flow direction of maritime air masses – revealed highest correlations ($r = 0.42$) between the RCS chronology and JJAS scPDSI data over the full period of proxy/target overlap (1901–2002). Note that similar correlations were found with the drought indices when using 300SP and NEG detrended chronologies, emphasizing that the RCS detrending – after horizontal data splitting – does not negatively impact the growth–climate relationship. Correlation decreased to 0.34 and increased to 0.49 over the first and second half of the calibration period, respectively (not shown). Overall

non-significant correlations were found for temperature. A more detailed view on potential wavelength-dependency of the JJAS drought signal indicated overall lower (higher) correlations of 0.4–0.42 (0.48–0.79) after 10–60-year high- (low-) pass filtering (Fig. 5B). Highest correlation of 0.84 was revealed after decadal-scale band-pass filtering (30–50 years), indicating that the strongest climate signal is retained at this frequency band. However, effects of increasing autocorrelation with decreasing frequencies on the degrees of freedom must be taken into account.

3.2. Model skill

Moving 31-year correlations between 20th century JJAS drought and oak growth indicated a period of reduced coherency in the mid-20th century and higher coherency towards the records' ends (Fig. 6A). Durbin–Watson (DW; Durbin and Watson, 1951) statistics ranging from 1.26 to 1.66 for the full and split periods tested for *lag-1* autocorrelation in the model residuals. A DW value of 2 means no 1st order autocorrelation in the residuals, whereas values greater (less) than 2 are indicative for negative (positive) autocorrelation. Annual residuals between the proxy and target data also displayed no overall trend ($r = 0.0001$; 1901–2002). After scaling the RCS
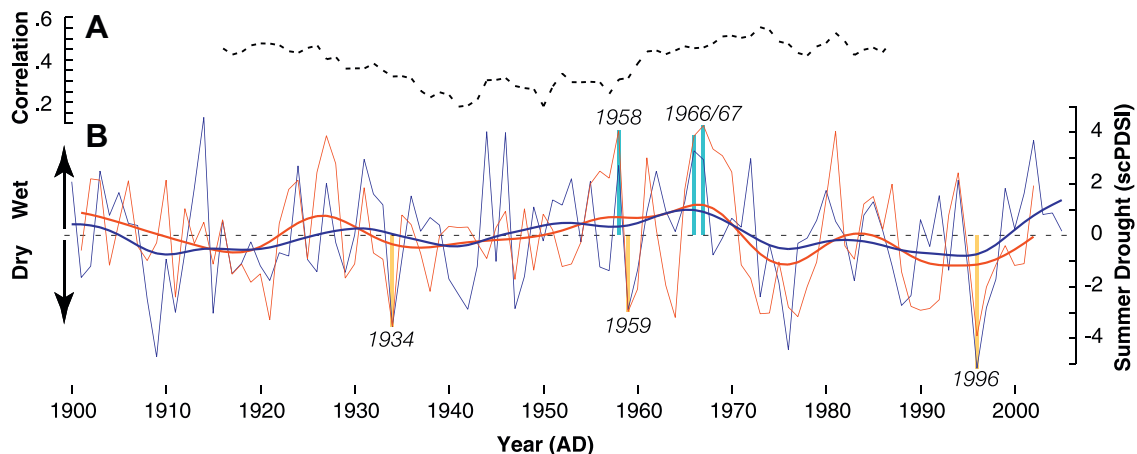
Fig. 6. Model skill: (A) 31-year moving correlations between (B) the scaled (1901–2002) RCS (blue) and JJAS scPDSI (red) time-series. The three most positive and negative years common to the proxy and target data are highlighted, and the bold curves are 20-year low-pass filters.

chronology against JJAS scPDSI indices over the full period of overlap (Fig. 6B), the model captured inter-annual to decadal scale variability, and the later was additionally emphasized by low-pass filtered time-series. The three driest summers commonly reflected by the TRW and scPDSI records were 1996, 1934, and 1959. The wettest growing seasons common to the proxy and target data occurred in 1958, 1966, and 1967. Fluctuations of dry (i.e., ∼1915–1920, 1935–1945, the 1970s, and the 1990s) and wet (i.e., ∼1925–1930, 1955–1970, and >2000) spells were reflected in both the reconstruction and instrumental time-series. Overall wetter summers in the 1980s were followed by a shift towards generally drier conditions until the late 1990s. Longer-term hydro-climatic trends during the calibration period were not obvious, neither in the target nor the proxy time-series.

3.3. Drought history

The JJAS scPDSI reconstruction reveals fairly dry conditions prior to ∼1200, two wet spells during the MCA in the 13th and 14th century, generally drier conditions (with respect to the 1961–1990 climatology) during the ∼1430–1720 LIA period, wetter summers between ∼1730 and 1800, and fairly moderate conditions over the past two centuries – in line with the instrumental target data (Fig. 7A). Superimposed on these long-term trends were decadal to multi-decadal fluctuations. The 20 wettest summers occurred between 1203–1362 and 1727–1797, whereas the 20 driest summers were found between 1010–1165 (associated with increased uncertainty) and 1420–1636. Inter-annual variability – showing similarities to the usual spread versus level relationship in raw TRW data (Frank et al., 2007b) – was higher during wet episodes, when growth indices showed high values and corresponded to increased soil-moisture availability from ∼1250 to 1350 and again from ∼1700 to 1900. Prolonged phases of desiccation, on the other hand, were associated with reduced high frequency variability (i.e., before ∼1200 and from ∼1450 to 1700). It remains unclear whether these spread-level relationships represent biases in the variance structure carried over from the raw TRW data or represent true changes in the variability of the earth's climate system (Frank et al., 2005). The record's early portion until ∼1300, during which average sample replication is relatively low
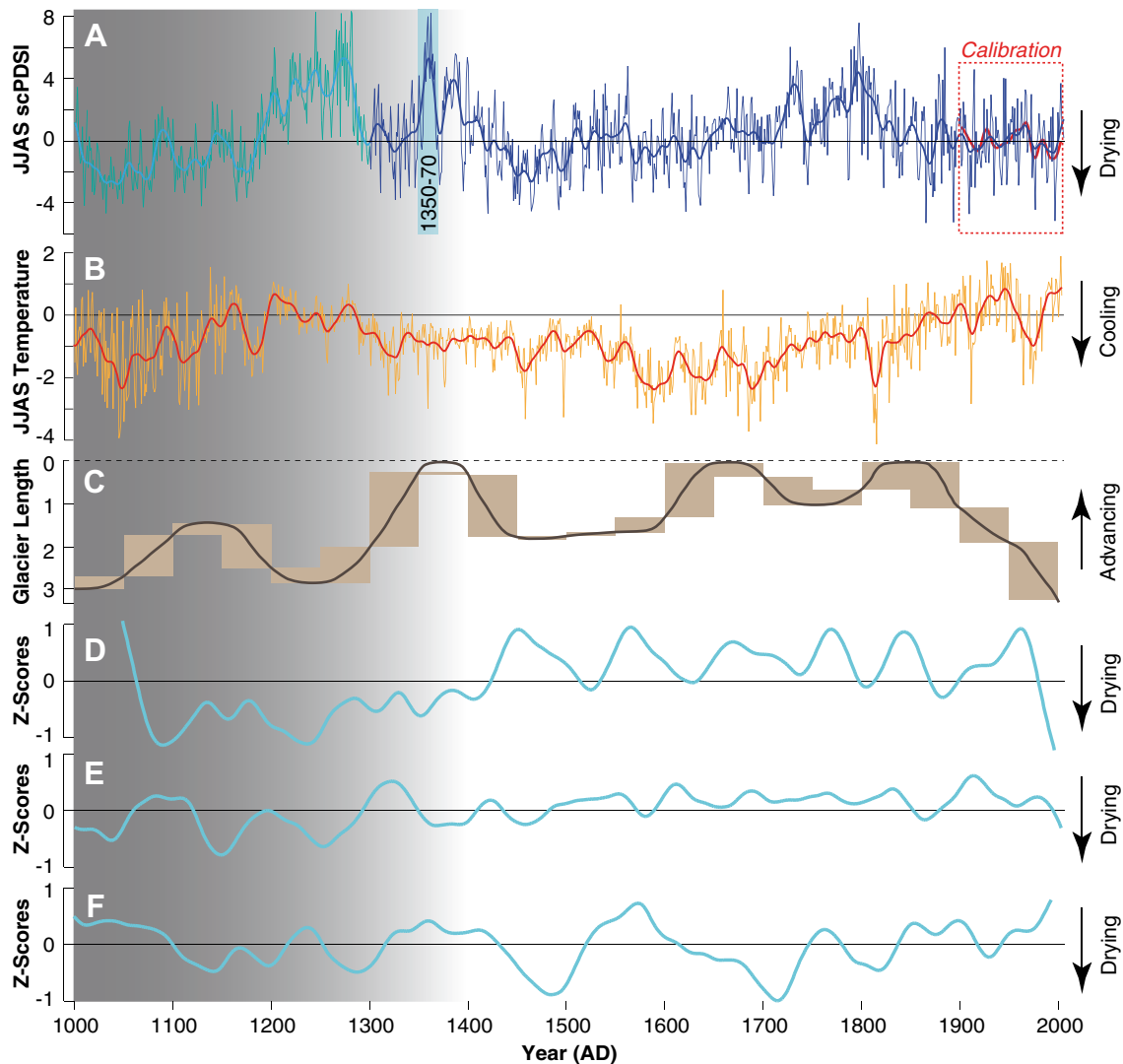
Fig. 7. Temporal variability: (A) Annually-resolved JJAS scPDSI reconstruction over the 996–2005 period, with the bold line being a 20-year low-pass filter. Blue horizontal bar indicates the 1350–1370 period of increased humidity. Light blue curves and the grey shading refer to increased uncertainty before AD 1300. (B) Alpine summer temperature variability (Büntgen et al., 2006), and (C) length fluctuation (m × 1000) and mass balance (50 year averages) of the Great-Aletsch glacier (Holzhauser et al., 2005). (D–F) TRW-based drought records from North Africa (Esper et al., 2007), North America (Cook et al., 2004), and East Asia (Sheppard et al., 2004) after 60 year smoothing.

(14 series), and EPS values drop below the commonly accepted quality threshold (<0.85) before 1050 and again $\sim$1285 (Fig. 2), is particularly prone to error.

3.4. Spatial signal

Spatial field correlation analysis between our reconstruction and gridded JJAS drought, precipitation, and cloud-cover data over the 1901–2002 (1950–2002 for cloud-cover) period revealed common spatial signatures (Fig. 8). The proxy record correlated significantly positively (>0.4) with scPDSI grid-box data over an apparent southwest-to-northeast corridor between western France and eastern Fennoscandia. Spatial field correlations are insignificant south of $\sim$48°N and for most of the western British Isles and western Scandinavia. Comparison between the oak data and precipitation totals showed slightly lower correlations largely restricted to Western and Central Europe, i.e., France, England, the Benelux, and Germany. Spatial field correlations using cloud-cover data (back to 1950) showed strongest agreement between oak growth and cloudiness over Great Britain and France. The same analysis using meteorological JJAS drought, precipitation, and cloud-cover data, instead of the oak-based indices, generally confirmed the proxy patterns: strong association with precipitation (cloud-cover) variability over Western Europe between 45 and 55°N (42–64°N), but no correlations east of $\sim$15°E. It is worth mentioning that the three meteorological parameters are interrelated and thus do not provide independent validation. Additional evidence for the heterogeneous nature of spatial precipitation (drought) variability can be derived from the weak high-frequency agreement of 12 TRW-based hydro-climatic proxy records distributed across the European/North Atlantic Sector (Fig. 9). While all records originate from temperate forest sites and contain significantly positive correlations with regional precipitation and drought variability (Fig. 9A), cross-correlation between the individual chronologies (and between nearby precipitation station readings) was found to be non-significant (Fig. 9B). Validation of the limited spatial significance of hydro-climatic proxy data at annual time-scales was provided by their spatial field correlations (Fig. 9C).

3.5. Synoptic circulation

Below-average Z500 values (Kalnay et al., 1996) over western-central Europe (centered over Ireland) were connected with the 10 wettest summers in Central Germany over the 20th century period of instrumental overlap (Fig. 10). Regional dry extremes, on the other hand, were induced by positive Z500 anomalies over the British Isles, Scandinavia and stretching over Germany, connected with subsidence and stability. This composite analysis was repeated using meteorological scPDSI data (rather than the proxy record) from the closest 0.5° × 0.5° grid-box to the study site, which displayed similar, but less distinct pressure fields (Fig. 10).

The spatial anomaly patterns for the 20 wettest and driest summer composites over the 1659–1900 period (Luterbacher et al., 2002) were less distinct than those over the 20th century. Above normal geopotential height anomalies over northeastern Europe (Finnish/Russian area) and a negative anomaly over the Icelandic region were connected with extremely wet summers during the past 350 years (Fig. 10). A positive Z500 area centered over the British Isles and northwestern France, in combination with negative geopotential height anomalies over northeastern Europe appears associated with dry summer conditions.

4. Discussion

4.1. Uncertainty assessment

Uncertainty inherent to millennium-long climate reconstructions based on composite TRW chronologies of living and historical data can derive from a weak growth/climate response, insecure frequency preservation, and changing forest structure and condition. Relationships between oak growth and summer drought (i), chronology development techniques and retained variance spectra
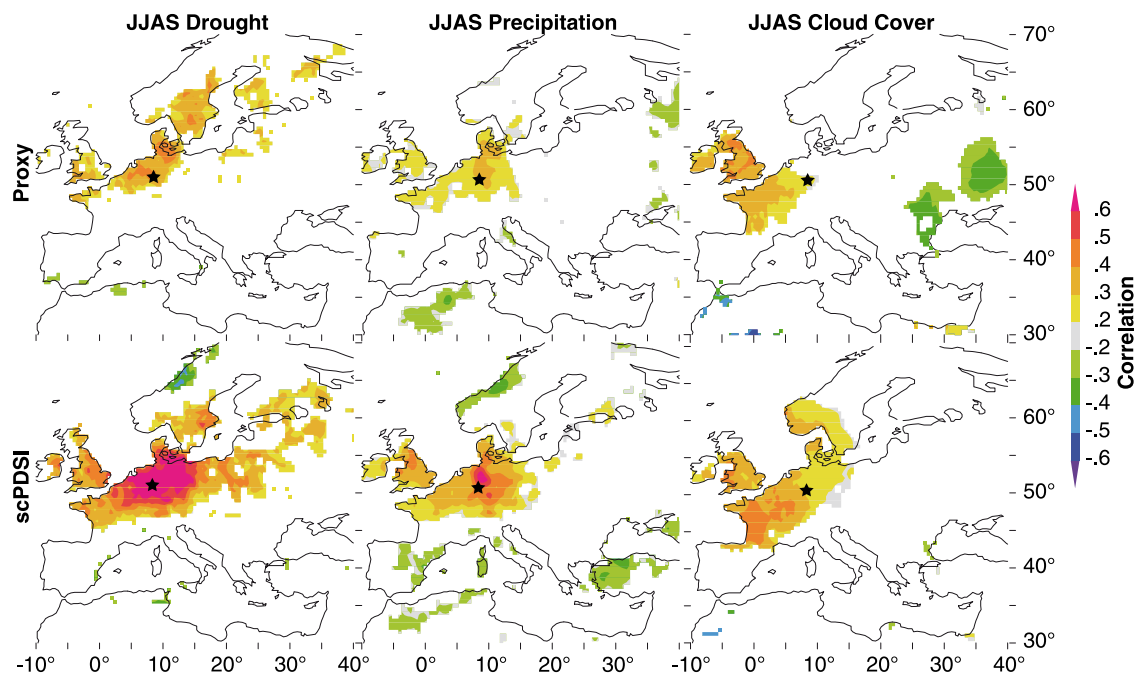
Fig. 8. Spatial significance: correlation of the reconstructed (upper) and measured (lower) scPDSI time-series (black star) against European-scale JJAS drought, precipitation (1901–2002) and cloud-cover (1950–2002) data (CRUTS2.1).
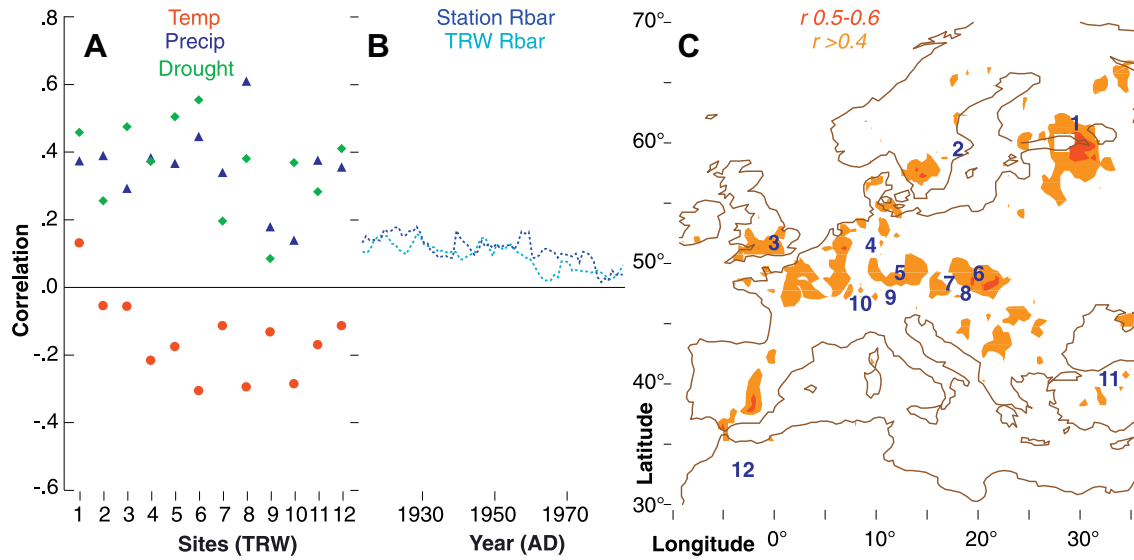
Fig. 9. Proxy signal: (A) Correlations (1901–1993) of 12 TRW-based hydro-climatic proxies and summer climate (June–August temperature, precipitation, scPDSI) of the closest grid-box. (B) Thirty-one-year moving inter-series correlation (Rbar) of the 12 proxy records and 12 nearby instrumental station readings. (C) Composite overlay of spatial correlations of the 12 proxy records using gridded summer scPDSI.

(ii), and effects of wood provenance, forest management, and site ecology (iii) are, therefore, assessed.

(i) Uncertainty in the relationship between the unfiltered proxy and target time-series is most likely related to the interaction of several climatic drivers (Nemani et al., 2003), and a complex physiology in temperate deciduous trees (Friedrichs et al., 2009a,b). Higher correlations on decadal time-scales suggest that noise is greater in the high-frequency domain. Nevertheless, the occurrence of pan-European annual extremes in TRW records – so-called pointer years – was previously explained by precipitation and temperature anomalies, associated with changing atmospheric circulation patterns (Kelly

et al., 2002), and a strong coherency between oak growth and drought was found in a more comprehensive time-series analysis (Friedrichs et al., 2009a,b). Threshold-induced response shifts or delayed reactions of tree growth to climate extremes, however, must be considered and most likely impact the high-frequency disassociation between the proxy and target time-series (Fig. 6B). On the other hand, indirect long-term effects of temperature variability and subsequent changes in growing season length, as well as plant physiological adaptation through the root system could impact oak growth in temperate forests. Note that some of the herein obtained model noise could also emerge from noise in the instrumental data themselves including the homogenization
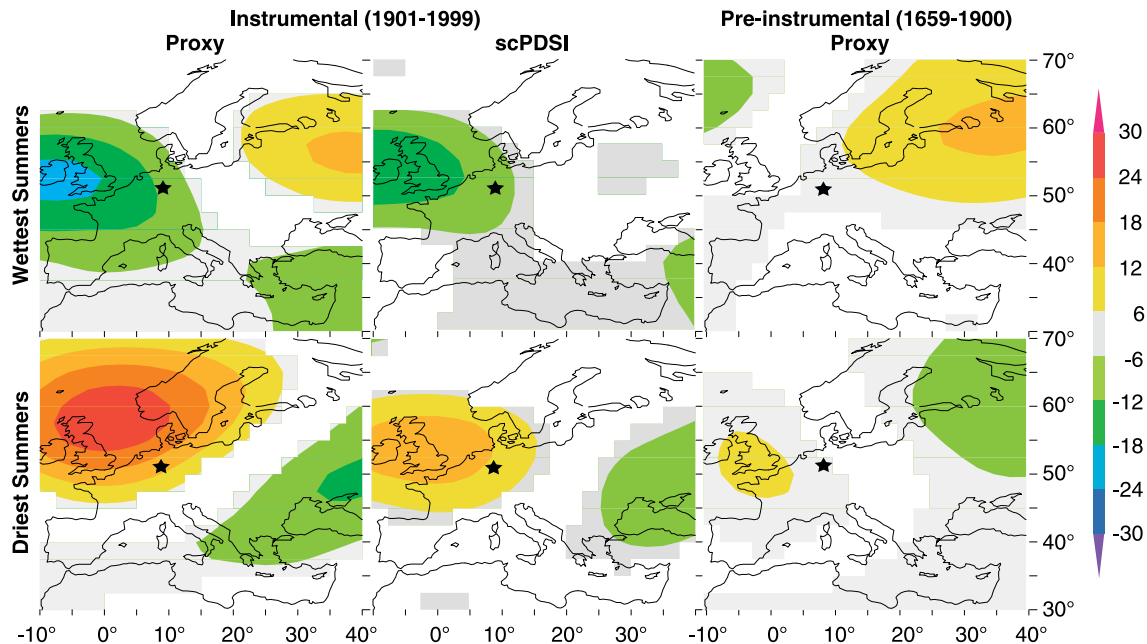
Fig. 10. Composite analysis: Z500 of the 10 wettest and driest summers of the proxy and instrumental scPDSI (1901–1999), as well as the 20 wettest and driest reconstructed summers over the pre-instrumental period (1659–1900). Black star indicates the study location.

and aggregation procedures applied to the gridded drought indices (Frank et al., 2007a). Methodological issues associated with the aggregation of such datasets could cause additional limitations in reflecting the full range of naturally to industrially forced climate variability (Mitchell and Jones, 2005).

(ii) Besides those biases that interfere with the proxy/target relationship, uncertainty in the overall course of our drought reconstruction complicates any long-term comparison between recent and medieval climatology. Possible error related to the tree-ring standardization and chronology development techniques applied, mainly affects the preserved low-frequency variability and subsequent amplitude range between pronounced dry and wet intervals (Esper et al., 2005). Inter-annual variability in the subset chronologies was separately stabilized using methods introduced by Frank et al. (2007b) to account for artificial variance changes over time, which can further impact the long-term evolution of any time-series. A time dependent '100-year moving window' approach for adjusting temporal changes in both sample replication and inter-series correlation was herein used. As a compromise between preserving sufficient low-frequency information while handling different tree populations over time (Helama et al., 2005), RCS was independently applied on three horizontal (living and historical) subsets, a strategy used for example by Büntgen et al. (2005). While this approach accounts for temporal changes in growth trends and levels, it still mitigates the so-called 'segment length curse' (Cook et al., 1995). Based upon the horizontal data splitting and the short segment length of the living trees, potential climate related variability during the instrumental period is restricted to inter-annual to multi-decadal time-scales, whereas during the historical period (~1300–1850), variability may exist to multi-centennial time-scales. Unfortunately, splitting the dataset likely does not allow recent mean drought conditions to be faithfully benchmarked with respect to the pre-industrial era. Despite those methodological limitations does decreasing sample size hinder robust conclusions to be drawn before ~1300, even though sufficient agreement between the individual TRW series exists back into medieval times (indicated by EPS values >0.85),

(iii) Uncertainty can also emerge from temporal changes in the precise understanding of wood provenance, changing forest management, and site ecology. Wood provenancing is generally complicated if archaeological remains (with short segments) are aggregated over larger areas (Haneca et al., 2009), but appears to be less problematic if construction timbers (with long segments) originate from spatially well-defined regions (see Wilson et al., 2004 for a detailed description of potential limitations to the use of historical TRW series for climate reconstructions). In this study, all samples could be re-traced down to parish level, because construction timbers were selected within a small area from which profound background information was available. Persistent parish forest size, supply and management strategies across Northern Hesse/Lower Saxony assured sufficient timber resources back to medieval times. The mountainous landscape and small river system of the study area limited wood transportation and floating over longer distances, with the net-weight of oak generally complicating floating activities. Altering forest management strategies that would cause non-climatic noise (see Haneca et al., 2009 for a review), as well as previously reported population shifts in sub-fossil European bog oaks (Leuschner et al., 2002), appear to be of minor importance as sample size was quite large over the past ~600 years, which naturally limits local-scale effects of forest management and population differences in the mean time-series. To further evaluate the robustness of the reconstructed drought swings associated with the MCA-LIA transition, application of various detrending methods, as well as precluding changing sample size and juvenile wood during the mid-14th century – where hydro-climatic pulses appeared to be most significant – were performed (Fig. 4). Varying site ecology over time (but also between the living sites) is also minimal, as the study area is relatively small, covered by homogeneous forest sites (Friedrichs et al., 2009a,b), and as site control and provenancing is maintained in the historical material back to medieval times.

4.2. Synoptic variability

Wet summers in Central Germany over the last century were characterized by an east–west dipole consisting of a cyclonic trough over the British Isles and a ridge over the Baltic region (Fig. 10). This is in agreement with the typical summer pressure distribution in Europe: a strong Azores high that extends towards central Europe and a rather weak Icelandic low. Hot and dry Central European summers are generally associated with prevailing high-pressure systems over the continent, which may result in strong subsidence and/or warm air advection from the southwest (Luterbacher et al., 2004). Thus, climatic summer conditions in Central Europe are mainly influenced by regional-scale processes, which are fairly sensitive to insulation patterns and lower boundary conditions associated with soil moisture (Luterbacher et al., 2000). Summer conditions are characterized by a dispersed convective precipitation pattern and small pressure gradients. At monthly and seasonal time-scales, advective processes are also of relevance to account for spatial well-constrained precipitation anomalies. Folland et al. (2009) recently reviewed the current state-of-the-art with respect to the effects of large-scale circulation dynamics on European summer climate, stressing the importance of the (summer) North Atlantic Oscillation. Our analysis indicates, that the occurrence of wet summers in Central Germany and over the last century was connected with anomalous westerly advection. This corresponds well to findings of Jacobeit et al. (2003), who analyzed the continuous evolution of atmospheric summer circulation not only with regard to frequency changes of major dynamical modes but also in terms of internal changes within each circulation mode concerning both dynamic properties in Central European temperature and precipitation over the past centuries. Our circulation pattern resembles the negative phase of the third Empirical Orthogonal Function (EOF) of atmospheric surface circulation over Europe (Slonosky et al., 2000), which implies anomalously strong cyclonic flow in the eastern Atlantic. This enhanced cyclonic flow is also illustrated by the increase in cloud-cover over the British Isles during wet summers in our record (Fig. 8). When the third EOF is in its positive phase, the meridional component of circulation over Europe is anomalously strong and a blocking high-pressure cell over northwestern Europe leads to enhanced northeasterly flow and dry conditions over most of the European continent (Barnston and Livezey, 1987). The cyclonic/blocking pattern west of the British Isles is most strongly expressed during winter months (Jacobeit et al., 2001, 2003; Luterbacher et al., 2002), but it has also been reported to imprint European temperature and precipitation patterns during other seasons (Casty et al., 2007).

Over the pre-instrumental period (1659–1900), an east–west dipole dominated by the eastern mode and the blocking high over the Baltic region, modulated the influence of the East Atlantic low-pressure system during wet summers (Fig. 10). This pressure pattern with an anticyclone center over the Baltic region has

previously been found to be the dominating mode of Central European LIA climate (Jacobeit et al., 1999), and specifically during the Late Maunder Minimum period (1675–1715; Luterbacher et al., 2001). During the second half of the 16th century, this pattern was associated with increased flood risks in Central Europe (Jacobeit et al., 2003). Our results confirm findings by Pauling et al. (2006), showing that this pattern consistently controlled precipitation over Central Germany during the period 1500–2002, whereas the cyclonic pattern over the British Isles has been leading mainly since 1850 only (see Fig. 6b in Pauling et al., 2006). It should, however, be noted that sufficient reconstruction skill has only been demonstrated from 1659 to present (Luterbacher et al., 2004), whereas increasing uncertainty and decreasing predictors were found during the first half of the 16th century.

4.3. Long-term perspective

The herein reconstructed Central German drought history provides a long-term perspective on hydro-climatic fluctuations for one of the most inhabited regions of Central Europe, characterized by high economic values of both agricultural and forest productivity. Our results support previously reported geomorphologic and documentary evidences for an extreme precipitation event, which caused an outstanding July flood and subsequent erosion in 1342 (Dotterweich and Bork, 2007). This heavy wet spell over the study area was most likely triggered by Vb (van Bebber) tracks of cyclones originating from the Mediterranean, and caused sustainable landscape changes of local- to regional-scale catchments across Central Germany (Bork and Kranz, 2008).

Cross-parameter comparison between our new drought reconstruction and Central European summer temperature variability based on maximum latewood density measurements from high-elevation trees in the Swiss Alps (Büntgen et al., 2006), allowed hydro-climatic dynamics to be discussed in the light of generally warm (MCA) versus cold (LIA) climate states (Fig. 7B). The slightly (negative) drying trend reconstructed for the past two centuries coincides the (positive) warming trend. Pluvial spells during the 18th century parallel the strong LIA cooling after a prolonged period of relative dry and cool conditions from ~1400 to 1700. Increased hydro-climatic variability occurred at the MCA to LIA transition characterized by a long-term decrease in European summer temperature. Data uncertainty before ~1300 is indicated by (artificial) variance inflation during the records' earlier portion (Frank et al., 2007b), calling for more data at the site- and network-level.

A broader perspective on the obtained drought history was derived from a comparison with length and mass balance fluctuations of the Great-Aletsch glacier (Holzhauser et al., 2005), which contain information of both, precipitation and temperature variability (Fig. 7C). Major glacier advances are evident during late medieval times (~1350–1400), the 17th century, and the first half of the 19th century – in line with fluctuations of the smaller Swiss Gorner glacier (not shown). Two major phases of glacier advance during the MCA and the 18th century – the latter corresponding to the Holocene maximum extent (Holzhauser et al., 2005) – were possibly driven by pluvial modes, but variations during the LIA were likely caused by modifications in atmospheric circulation patterns (Raible et al., 2007). It has been demonstrated that relatively dry but cold conditions occurred during most of the Maunder Minimum (Luterbacher et al., 2001). Nevertheless, temporal changes in the relevant fraction of precipitation, temperature, and/ or solar forcing on Alpine glacier fluctuations, as well as their time lag in response to climate variability, must be taken into account, particularly when comparing higher frequency (decadal) fluctuations amongst different proxy archives (Holzhauser et al., 2005). On the other hand, glacier records add unique information towards a better understanding of longer-term amplitude changes in the earth's climate system (Oerlemans, 2005).

Three available TRW-based drought reconstructions of millennium-length that originate from North Africa (Esper et al., 2007), North America (Cook et al., 2004), and East Asia (Sheppard et al., 2004), were used for a (proxy-internal) long-term comparison of hydro-climatic variability at different geographical locations across the Northern Hemisphere (Fig. 7D–E). Hoerling and Kumar (2003) were the first who recognized a zonal pattern of symmetric mid-latitudinal dryness that dynamically linked the late 20th century droughts in North America, the Mediterranean, and Central Asia, and Schubert et al. (2004) demonstrated that there is additional hemispheric symmetry of regional drought spells. Their global footprint and hemispheric symmetry suggest causes to be found in the tropics (see Cook et al., 2007 for a review of possible drought mechanisms). Opposing variability in Germany and Morocco, particularly in the 13th through 17th century, reflects a climatic dipole across Northern/Central Europe and North Africa. This pattern confirms previously reported pluvial (dry) MCA (LIA) conditions at higher latitudes, contrasting with medieval drought but a relative humid LIA in the tropics (see Trouet et al., 2009 for a synoptic description). Evidence for pluvial MCA swings was also reported by Lamb (1965) and Proctor et al. (2000) for northwest Europe, and by Treydte et al. (2006) and Sheppard et al. (2004) for Southwest and East Asia, respectively. In contrast, severe droughts – in line with Esper et al. (2007) – were reported for western North America (Cook et al., 2004), and for eastern (Sinha et al., 2007) and equatorial (Verschuren et al., 2000) Africa. Some of these hydro-climatic fluctuations are hypothesized to be associated with a La Niña-like atmospheric state (Graham et al., 2007), and a related persistent North Atlantic Oscillation dipole structure during medieval times (Trouet et al., 2009), for which external solar forcing, internal oscillations, and more complex ocean-atmosphere feedbacks were most likely responsible. Most recent evidence for increased La Niña-like MCA climate stages paced by positive tropical radiative forcing of high solar irradiance and inactive tropical volcanism derives from a global proxy network (Mann et al., 2009). In this regard, it might be worth mentioning that heterogeneous patterns of medieval climate variability were not only postulated for precipitation, but also for temperature (Bradley et al., 2003; but see also Esper and Frank, 2009). At this stage, we are, however, unable to link the observed hydro-climatic fluctuations at hemispheric-scale with plausible physical factors, although the majority of forcing hypotheses described thus far relies on interactions within to the earth's climate system, or relies on external solar variations and changes in volcanic aerosols. Interestingly, it has been argued that even though the solar forcing signal upon the global temperature is of very small size, associated effects on the amplitude of decadal sea-surface temperature (SST) anomalies might be strong enough to cause major droughts (see Cook et al., 2007 and references therein). For details on larger-scale climate dynamics and potential forcing agents during the MCA-LIA transition, we also refer to recent work by Emile-Geay et al. (2007) and Seager et al. (2007), nevertheless we are aware that much more proxy records, not only of hydro-climatic but also of temperature sensitivity are necessary to enhance our understanding of dynamical processes of natural climate variability. Additional insight might stem from model simulations (e.g., Zorita et al., 2005), as well as Proxy Surrogate Reconstruction techniques (PSR; Graham et al., 2007), which are analogue methods based on proxy-model similarity, allowing not only to describe past climate states but also to evaluate the required proxy number and locations necessary to reconstruct large-scale climate variability. Palaeooceanograpic evidence of decadal-scale variations in North

Atlantic SST and salinity might also provide an additional perspective on the possible drivers of natural climate variability over the past millennium (e.g., Lund et al., 2006). The Atlantic Meridional Overturning Circulation (AMOC), for example, can generate a cross-equatorial SST gradient and changes in the Inter-Tropical Convergence Zone (ITCZ), and can thus function as an amplifier of external forcing that is further modified by internal oscillations (Bianchi and McCave, 1999).

It should be noted that late medieval times were not only unique from a climatic perspective, but also from a social point of view. In fact, the 'Black Death' plague pandemic decimated Medieval Europe, with major impacts on the continent's socio-economic development, culture, art, religion, and politics, as 40–60% of the population was reduced after 1347 (Stenseth et al., 2008). A robust link between plague outbreaks and climate variability has so far only been reported for Central Asia and the 20th century (Stenseth et al., 2006). Interdisciplinary research, therefore, demands focus on climatic (spring–summer drought/humidity), environmental (forest cover), and socio-cultural (famine) circumstances during medieval (14th century) Europe, searching for potential external drivers of the world's largest pandemic threat.

5. Conclusions

A dataset of 953 living and historical oak TRW samples from central-west Germany was compiled. Calibrated against JJAS scPDSI data, the model explained 18–70% of annual-decadal summer drought variability over the period 1901–2002. Particular dry conditions occurred before ∼1200, though oak sample replication and related chronology robustness are quite low during this early period of the past millennium. Pluvial pulses dominated the 13th and 14th centuries. Overall drier conditions were reconstructed for most of the LIA between ∼1430 and 1720, whereas wetter summers and fairly moderate conditions were characteristic for ∼1730–1800. Due to the separate detrending of living and historical material, it remains challenging to benchmark present conditions during the past century again these pre-industrial variations. Mid-tropospheric high pressure over the North Sea and low pressure over southeastern Europe triggered reconstructed summer droughts. In contrast, below normal pressure centered over the British Isles and anomalous positive pressure anomalies over northeastern Europe were associated with the wet summer conditions in our study area. We provided a new line of evidence for Central European hydro-climatic variability back into the MCA. Our study demonstrated the strength of carefully selected living and historical oak trees to reconstruct regional-scale drought dynamics.

Acknowledgements

References

Barnston, A.G., Livezey, R.E., 1987. Classification, seasonality and persistence of low-frequency atmospheric circulation patterns. Monthly Weather Reviews 115, 1083–1126.
Bianchi, G.G., McCave, I.N., 1999. Holocene periodicity in North Atlantic climate and deep-ocean flow south of Iceland. Nature 397, 515–517.
Brázdil, R., Štěpánková, P., Kyncl, T., Kyncl, J., 2002. Fir tree-ring reconstruction of March–July precipitation in southern Moravia (Czech Republic), 1376–1996. Climatic Research 20, 223–239.
Brázdil, R., Pfister, C., Wanner, H., von Storch, H., Luterbacher, J., 2005. Historical climatology in Europe—the state of the art. Climatic Change 70, 363–430.
Bork, H.R., Kranz, A., 2008. Die Jahrtausendflut des Jahres 1342 prägt Deutschland. Naturkunde 158, 119–129.
Bradley, R.S., Hughes, M.K., Diaz, H.F., 2003. Climate in medieval times. Science 302, 404–405.
Büntgen, U., Esper, J., Frank, D.C., Nicolussi, K., Schmidhalter, M., 2005. A 1052-year tree-ring proxy of Alpine summer temperatures. Climate Dynamics 25, 141–153.
Büntgen, U., Frank, D.C., Nievergelt, D., Esper, J., 2006. Summer temperature variations in the European Alps, AD 755–2004. Journal of Climate 19, 5606–5623.
Büntgen, U., Frank, D.C., Grudd, H., Esper, J., 2008. Long-term summer temperature variations in the Pyrenees. Climate Dynamics 31, 615–631.
Büntgen, U., Brázdil, R., Frank, D.C., Esper, J., 2009. Three centuries of Slovakian drought dynamics. Climate Dynamics. doi:10.1007/s00382-009-0563-2.
Casty, C., Raible, C.C., Stocker, T.F., Wanner, H., Luterbacher, J., 2007. A European pattern climatology 1766–2000. Climate Dynamics 29, 791–805.
Cook, E.R., Peters, K., 1981. The smoothing spline: a new approach to standardizing forest interior tree-ring width series for dendroclimatic studies. Tree-Ring Bulletin 41, 45–53.
Cook, E.R., Peters, K., 1997. Calculating unbiased tree-ring indices for the study of climatic and environmental change. The Holocene 7, 361–370.
Cook, E.R., Briffa, K.R., Meko, D.M., Graybill, D.A., Funkhouser, G., 1995. The 'segment length curse' in long tree-ring chronology development for palaeoclimatic studies. The Holocene 5, 229–237.
Cook, E.R., Woodhouse, C., Eakin, C.M., Meko, D.M., Stahle, D.W., 2004. Long-term aridity changes in the western United States. Science 306, 1015–1018.
Cook, E.R., Seager, R., Cane, M.A., Stahle, D.W., 2007. North American drought: reconstructions, causes, and consequences. Earth-Science Reviews 81, 93–134.
Dotterweich, M., Bork, H.R., 2007. Jahrtausendflut 1342. Archäologie in Deutschland 4, 38–40.
Durbin, J., Watson, G.S., 1951. Testing for serial correlation in least squares regression. Biometrika 38, 159–178.
Emile-Geay, J., Cane, M., Seager, R., Kaplan, A., Almasi, P., 2007. El Nino as a mediator of the solar influence on climate. Paleoceanography 22. doi:10.1029/2006PA001304.
Esper, J., Cook, E.R., Krusic, P.J., Peters, K., Schweingruber, F.H., 2003. Tests of the RCS method for preserving low-frequency variability in long tree-ring chronologies. Tree-Ring Research 59, 81–98.
Esper, J., Frank, D.C., Wilson, R.J.S., Briffa, K.R., 2005. Effect of scaling and regression on reconstructed temperature amplitude for the past millennium. Geophysical Research Letters 32. doi:10.1029/2004GL021236.
Esper, J., Frank, D., Büntgen, U., Verstege, A., Luterbacher, J., Xoplaki, E., 2007. Long-term drought severity variations in Morocco. Geophysical Research Letters 34. doi:10.1029/2007GL030844.
Esper, J., Frank, D.C., 2009. The IPCC on a heterogeneous Medieval Warm Period. Climatic Change 94, 267–273.
Folland, C.F., Knight, J., Linderholm, H.W., Fereday, D., Ineson, S., Hurrell, J.W., 2009. The summer North Atlantic oscillation: past, present, and future. Journal of Climate 22, 1082–1103.
Frank, D., Wilson, R.J.S., Esper, J., 2005. Synchronous variability changes in alpine temperature and tree-ring data over the last two centuries. Boreas 34, 498–505.
Frank, D., Büntgen, U., Böhm, R., Maugeri, M., Esper, J., 2007a. Warmer early instrumental measurements versus colder reconstructed temperatures: shooting at a moving target. Quaternary Science Reviews 26, 3298–3310.
Frank, D., Esper, J., Cook, E.R., 2007b. Adjustment for proxy number and coherence in a large-scale temperature reconstruction. Geophysical Research Letters 34. doi:10.1029/2007GL030571.
Friedrichs, D., Büntgen, U., Esper, J., Frank, D., Neuwirth, B., Löffler, J., 2009a. Complex climate controls on 20th century oak growth in central-west Germany. Tree Physiology 29, 39–51.
Friedrichs, D., Trouet, V., Büntgen, U., Frank, D.C., Esper, J., Neuwirth, B., Löffler, J., 2009b. Twentieth century climate sensitivity of Central European tree species. Trees, Structure and Function 23, 729–739.
Graham, N.E., Hughes, M.K., Ammann, C.A., Cobb, K.M., Hoerling, M.P., Kennett, D.J., Kennett, J.P., Rein, B., Stott, L., Wigand, P.E., Xu, T., 2007. Tropical Pacific—mid-latitude teleconnections in medieval times. Climatic Change 83, 241–285.
Grove, J.M., 1988. The Little Ice Age. Methuen & Co..
Haneca, K., Čufar, K., Beeckman, H., 2009. Oaks, tree-rings and wooden cultural heritage: a review of the main characteristics and applications of oak dendrochronology in Europe. Journal of Archaeological Science 36, 1–11.
Helama, S., Timonen, M., Lindholm, M., Merilainen, J., Eronen, M., 2005. Extracting long-period climate fluctuations from tree-ring chronologies over timescales of centuries to millennia. International Journal of Climatology 25, 1767–1779.
Helama, S., Meriläinen, J., Tuomenvirta, H., 2009. Multicentennial megadrought in northern Europe coincided with a global El Niño–Southern Oscillation drought pattern during the Medieval Climate Anomaly. Geology 37, 175–178.
Hoerling, M., Kumar, A., 2003. The perfect ocean of drought. Science 299, 691–694.
Holzhauser, H., Magny, M., Zumbühl, H.J., 2005. Glacier and lake-level variations in west-central Europe over the last 3500 years. The Holocene 15, 789–801.
Huntington, T.G., 2006. Evidence for intensification of the global water cycle: review and synthesis. Journal of Hydrology 319, 83–95.

Jacobeit, J., Wanner, H., Koslowski, G., Gudd, M., 1999. European surface pressure patterns for months with outstanding climatic anomalies during the sixteenth century. Climatic Change 43, 201–221.

Jacobeit, J., Jönsson, P., Bärring, L., Beck, C., Ekström, M., 2001. Zonal indices for Europe 1780–1995 and running correlations with temperature. Climatic Change 48, 219–241.

Jacobeit, J., Wanner, H., Luterbacher, J., Beck, C., Philipp, A., Sturm, K., 2003. Atmospheric circulation variability in the North-Atlantic-European area since the mid-seventeenth century. Climate Dynamics 20, 341–352.

Kalnay, E., Kanamitsu, M., Kistler, R. and 19 co-authors, 1996. The NCEP/NCAR 40-Year reanalysis project. Bulletin of the American Meteorological Society 77, 437–470.

Kelly, P.M., Munro, M.A.R., Hughes, M.K., Goodess, C.M., 1989. Climate and signature years in west European oaks. Nature 340, 57–60.

Kelly, P.M., Leuschner, H.H., Briffa, K.R., Harris, I.C., 2002. The climatic interpretation of pan-European signature years in oak ring-width series. The Holocene 12, 689–694.

Lamb, H.H., 1965. The early medieval warm epoch and its sequel. Palaeogeography, Palaeoclimatology, Palaeoecology 1, 13–37.

Leuschner, H.H., Sass-Klaassen, U., Jansma, E., Baillie, M.G.L., Spurk, M., 2002. Subfossil European bog oaks: population dynamics and long-term growth depressions as indicators of changes in the Holocene hydro-regime and climate. The Holocene 6, 695–706.

Lund, D.C., Lynch-Stieglitz, J., Curry, W.B., 2006. Gulf Stream density structure and transport during the past millennium. Nature 444, 601–604.

Luterbacher, J., Rickli, C., Tinguely, E. and 31 co-authors, 2000. Reconstruction of monthly mean sea level pressure over Europe for the Late Maunder Minimum period (1675–1715). International Journal of Climatology 20, 1049–1066.

Luterbacher, J., Rickli, R., Xoplaki, E., Tinguely, C., Beck, C., Pfister, C., Wanner, H., 2001. The Late Maunder Minimum (1675–1715)—a key period for studying decadal scale climate change in Europe. Climatic Change 49, 441–462.

Luterbacher, J., Xoplaki, E., Dietrich, D., Rickli, R., Jacobeit, J., Beck, C., Gyalistras, D., Schmutz, C., Wanner, H., 2002. Reconstruction of sea level pressure fields over the Eastern North Atlantic and Europe back to 1500. Climate Dynamics 18, 545–561.

Luterbacher, J., Dietrich, D., Xoplaki, E., Grosjean, M., Wanner, H., 2004. European seasonal and annual temperature variability, trends and extremes since 1500 A.D. Science 303, 1499–1503.

Mann, M.E., Zhang, Z., Rutherford, S., Bradley, R.S., Hughes, M.K., Shindell, D., Ammann, C., Faluvegi, G., Ni, F., 2009. Global signatures and dynamical origins of the little ice age and medieval climate anomaly. Science 326, 1256–1260.

Mitchell, T.D., Jones, P.D., 2005. An improved method of constructing a database of monthly climate observations and associated high-resolution grids. International Journal of Climatology 25, 693–712.

Nemani, R.R., Keeling, C.D., Hashimoto, H., Jolly, W.M., Piper, S.C., Tucker, C.J., Myneni, R.B., Running, S.W., 2003. Climate-driven increases in global terrestrial net primary production from 1982 to 1999. Science 300, 1560–1563.

Oerlemans, J., 2005. Extracting a climate signal from 169 glacier records. Science 308, 675–677.

Pauling, A., Luterbacher, J., Casty, C., Wanner, H., 2006. 500 Years of gridded high-resolution precipitation reconstructions over Europe and the connection to large-scale circulation. Climate Dynamics 26, 387–405.

Proctor, C.J., Baker, A., Barnes, W.L., Gilmour, M.A., 2000. A thousand year speleothem proxy record of North Atlantic climate from Scotland. Climate Dynamics 16, 815–820.

Raible, C.C., Yoshimori, M., Stocker, T.F., Casty, C., 2007. Extreme midlatitude cyclones and their implications to precipitation and wind speed extremes in simulations of the Maunder Minimum versus present day conditions. Climate Dynamics 28, 409–423.

Schubert, S.D., Suarez, M.J., Region, P.J., Koster, R.D., Bacmeister, J.T., 2004. On the cause of the 1930s Dust Bowl. Science 303, 1855–1859.

Seager, R., Graham, N., Herweijer, C., Gordon, A.L., Kushnir, Y., Cook, E., 2007. Blueprints for Medieval hydroclimate. Quaternary Science Reviews 26, 2322–2336.

Sheppard, P.R., Tarasov, P.E., Graumlich, L.J., Heussner, K.U., Wagner, M., Österle, H., Thompson, L.G., 2004. Annual precipitation since 515 BC reconstructed from living and fossil juniper growth of northeastern Qinghai Province, China. Climate Dynamics 23, 869–881.

Sinha, A., Cannariato, K.G., Stott, L.D., Cheng, H., Edwards, R.L., Yadava, M.G., Ramesh, R., Singh, I.B., 2007. A 900-year (600–1500 A.D.) record of the Indian summer monsoon precipitation from the core monsoon zone of India. Geophysical Research Letters 34. doi:10.1029/2007GL030431.

Slonosky, V.C., Jones, P.D., Davies, T.D., 2000. Variability of the surface atmospheric circulation over Europe, 1774–1995. International Journal of Climatology 20, 1875–1897.

Stenseth, N.C., Atshabar, B.B., Begon, M., Belmain, S.R., Bertherat, E., Carniel, E., Gage, K.L., Leirs, H., Rahalison, L., 2008. Plague: past, present, and future. PLOS Medicine 5. doi:10.1371/journal.pmed.0050003.

Stenseth, N.C., Samia, N.I., Viljugrein, H., Kausrud, K.L., Begon, M., Davis, S., Leirs, H., Dubyanskiy, V.M., Esper, J., Ageyev, V.S., Klassovskiy, N.L., Pole, S.B., Chan, K.S., 2006. Plague dynamics are driven by climate variation. Proceedings of the National Academy of Science 103, 13110–13115.

Touchan, R., Xoplaki, E., Funkhouser, G., Luterbacher, J., Hughes, M.K., Erkan, N., Akkemik, Ü., Stephan, J., 2005. Reconstructions of spring/summer precipitation for the Eastern Mediterranean from tree-ring widths and its connection to large-scale atmospheric circulation. Climate Dynamics 25, 75–98.

Treydte, K., Schleser, G.H., Helle, G., Frank, D.C., Winiger, M., Haug, G.H., Esper, J., 2006. The twentieth century was the wettest period in northern Pakistan over the past millennium. Nature 440, 1179–1182.

Trouet, V., Esper, J., Graham, N.E., Baker, A., Scourse, J.D., Frank, D.C., 2009. Persistent positive North Atlantic Oscillation mode dominated the Medieval Climate Anomaly. Science 324, 78–80.

van der Schrier, G., Briffa, K.R., Jones, P.D., Osborn, T.J., 2006. Summer moisture variability across Europe. Journal of Climate 19, 2818–2834.

Verschuren, D., Laird, K.R., Cumming, B.F., 2000. Rainfall and drought in equatorial east Africa during the past 1100 years. Nature 403, 410–414.

Wigley, T.M.L., Briffa, K.R., Jones, P.D., 1984. On the average of value of correlated time series, with applications in dendroclimatology and hydrometeorology. Journal of Climatology and Applied Meteorology 23, 201–213.

Wilson, R.J.S., Esper, J., Luckman, B.H., 2004. Utilising historical tree-ring data for dendroclimatology: a case Study from the Bavarian Forest, Germany. Dendrochronologia 21, 53–68.

Wilson, R.J.S., Luckman, B.H., Esper, J., 2005. A 500-year dendroclimatic reconstruction of spring/summer precipitation from the lower Bavarian Forest Region, Germany. International Journal of Climatology 25, 611–630.

Zhang, X., Zwiers, F.W., Hegerl, G.C., Lambert, F.H., Gillett, N.P., Solomon, S., Stott, P.A., Nozawa, T., 2007. Detection of human influence on twentieth-century precipitation trends. Nature 448, 461–465.

Zorita, E., González-Rouco, J.F., von Storch, H., Montávez, J.P., Valero, F., 2005. Natural and anthropogenic modes of surface temperature variations in the last thousand years. Geophysical Research Letters 32. doi:10.1029/2004GL021563.